Lithium Metal Anodes

International Edition: DOI: 10.1002/anie.201907759
German Edition: DOI: 10.1002/ange.201907759

Highly Stable Lithium Metal Anode Interface via Molecular Layer Deposition Zircone Coatings for Long Life Next-Generation Battery Systems

Keegan R. Adair, Changtai Zhao, Mohammad Norouzi Banis, Yang Zhao, Ruying Li, Mei Cai, and Xueliang Sun**

Abstract: *Herein, molecular layer deposition is used to form a nanoscale "zircone" protective layer on Li metal to achieve stable and long life Li metal anodes. The zircone-coated Li metal shows enhanced air stability, electrochemical performance and high rate capability in symmetrical cell testing. Moreover, as a proof of concept, the protected Li anode is used in a next-generation Li-O_2 battery system and is shown to extend the lifetime by over 10-fold compared to the batteries with untreated Li metal. Furthermore, in-situ synchrotron X-ray absorption spectroscopy is used for the first time to study an artificial SEI on Li metal, revealing the electrochemical stability and lithiation of the zircone film. This work exemplifies significant progress towards the development and understanding of MLD thin films for high performance next-generation batteries.*

Li metal anodes have recently gathered significant interest due to their high specific capacity (3860 $mAh\,g^{-1}$) and low electrochemical potential (−3.04 V vs. standard hydrogen electrode). The use of Li metal as an anode material is required for several next-generation energy storage systems such as Li-S and Li-O_2 batteries. However, the unstable solid-electrolyte interphase (SEI),[1] large volume fluctuations,[2] and dendrite growth[3] have caused serious safety concerns and inhibited the commercialization of Li metal batteries. The formation of inhomogeneous SEI components on the surface of Li metal can cause non-uniform Li-ion flux, leading to uneven Li plating/stripping and eventual dendrite growth. Moreover, the low Coulombic efficiency of Li metal anodes can often be attributed to the formation of inactive Li deposits, which leads to large voltage polarizations and cell failure. Therefore, the Li metal anode must be stabilized to achieve long life and safe Li metal batteries.

Various strategies have been proposed to stabilize the Li metal anode, including the development of 3D hosts,[4] electrolyte additives,[5] and artificial protection layers.[6] Among them, atomic layer deposition (ALD) and molecular layer deposition (MLD) have been shown to be excellent gas-phase thin film deposition techniques due to their ability to precisely control film thickness and composition at the atomic level.[7] The self-limiting reaction mechanisms involved in MLD are ideal for the fabrication of artificial SEI layers which can prevent side reactions between Li metal and electrolyte, thus improving Coulombic efficiency and cycling stability.

Herein, we demonstrate the application of MLD zircone on Li metal for high performance Li metal batteries. The zircone coating shows significantly improved rate capability and cycling performance compared to previously developed ALD/MLD coatings, and the stability is demonstrated in a next-generation Li-O_2 battery system. Moreover, we utilize in situ X-ray absorption near edge structure (XANES) for the first time to analyze the SEI on a Li metal surface, showing the electrochemical stability and lithiation of the zircone coating on Li metal. This work will provide new insight into the development of nanoscale interfacial coatings for Li metal and demonstrates new techniques for the analysis of protection coatings on a Li metal surface.

Figure 1 A shows an illustration of the deposited MLD zircone film on a Li metal anode. The metalcone coating was deposited at 130 °C using alternating pulses of zirconium tert-butoxide and ethylene glycol according to previous reports.[8] In this study, the thickness of the nanoscale interfacial coatings were tuned by the number of MLD subcycles (10, 25, 50 cycles) and denoted as Li@10ZrEG, Li@25ZrEG, and Li@50ZrEG, respectively. The deposition of MLD zircone on Li metal was initially confirmed by time-of-flight mass spectrometry depth profiling (ToF-SIMs), as seen in Figure 1 B. In the near surface region there is a high concentration of organic CH^- species from the ethylene glycol organic bridging ligands attached to the zirconium metal center. Moreover, $ZrCOH^-$ fragments can be detected, which is consistent with the structure of MLD zircone. As the sputtering time increases, the plateaus associated with $ZrCOH^-$ and CH^- begin to drop off, indicating the interface between the zircone coating and Li metal has been reached. In addition, the concentration of Li^- species increases with sputtering time, which indicates the presence of an artificial thin film coating on the outer surface. Furthermore, the chemical ion species images are displayed in Figure 1 D and confirms that the bulk Li had been reached by the end of the tested sputtering time. The sputtering rate of $\approx 0.25\,nm\,s^{-1}$

[*] K. R. Adair, C. Zhao, M. N. Banis, Y. Zhao, R. Li, X. Sun
Department of Mechanical and Materials Engineering
University of Western Ontario
London, Ontario N6A 5B9 (Canada)
E-mail: xsun@eng.uwo.ca
M. Cai
General Motors R&D Center
Warren, MI 48090-9055 (USA)
E-mail: mei.cai@gm.com
Supporting information and the ORCID identification number(s) for the author(s) of this article can be found under https://doi.org/10.1002/anie.201907759.

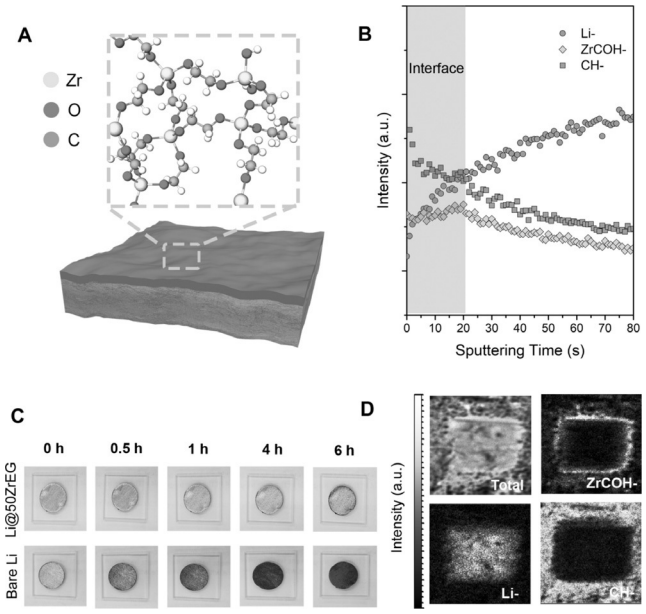

Figure 1. A) Illustration of a protective zircone coating on a Li metal anode. B) ToF-SIMs depth profiling of MLD zircone on Li metal and D) chemical ion images for $ZrCOH^-$, Li^-, and CH^- species. C) Optical images of bare Li and zircone-coated Li metal after exposure to air at different time intervals.

corresponds to a zircone coating of approximately 5 nm thick, which is in line with the previously reported literature on MLD zircone growth rates in this temperature regime.[8,9]

Air stability and processability are also important factors to consider for the design of practical Li metal batteries.[10] The reactive nature of Li metal under ambient conditions causes serious safety concerns and can lead to the formation of undesirable interfacial reaction products that can degrade electrochemical performance. Therefore, the fabrication of Li metal anodes with improved air-stability are greatly desired for the scale-up and mass production of Li metal batteries. The air stability of zircone-coated Li metal was compared to the untreated Li metal, as displayed in Figure 1 C. It can be seen that the untreated Li metal quickly oxidizes and reacts with components such as CO_2, N_2, H_2O, and O_2 present in the ambient atmosphere. Without any pretreatment, the bare Li metal is unsuitable for manufacturing outside a glovebox. However, the zircone-coated Li metal shows significant enhancement in air stability, with little tarnish being visible until approximately 6 h of exposure. The electronic structure of the zircone coating was also explored through analysis of the Zr L_3-edge XANES spectra before and after exposure to air for ≈2 h (Figure S1). The peaks of the Zr L_3-edge spectra correspond to the 2p→4d transition where the spectral shapes are affected by the density of unoccupied 4d states. Thus, any change in the bonding structure of the zircone coating after air exposure would lead to significant changes in the electronic transitions and spectral features. After 2 h of air exposure at a pressure of 10 torr, little difference can be found in the Zr L_3 features, suggesting good chemical stability towards components in the air. Moreover, it has been previously indicated that in contrast to MLD alucone, zircone is more air stable, which can explain its improved performance as a physical and chemical barrier for Li metal anodes.[8,11]

To understand the effects of the number of MLD zircone cycles on the electrochemical performance, symmetrical Li || Li and Cu || Li cells were fabricated. The Coulombic efficiencies of cells with zircone coatings were found to be significantly improved over those using bare Cu as the anode, regardless of the number of coating cycles (Figure S2). An average Coulombic efficiency as high as 97.7 % was achieved over the first 80 cycles for the protected anodes, whereas the bare Cu cells displayed an average Coulombic efficiency of 96.7 % before undergoing rapid performance degradation. However, the difference in electrochemical performance of the zircone coatings becomes more apparent when conducting Li || Li symmetrical cell tests. Figure S3 displays the cycling performance of the zircone-coated Li metal symmetric cells at a current density of 3 mA cm^{-2} with a capacity of 1 mAh cm^{-2} in carbonate-based electrolyte. It quickly becomes apparent that the electrochemical performance of the protected Li metal anodes is far superior to that of the bare Li metal with greatly extended cycle life at a high current density. The best electrochemical performance is achieved with 25 cycles of MLD zircone, which is capable of over 200 cycles with minimal increase in overpotential and improved stability. It is likely that 25 cycles of zircone is enough to achieve a complete and uniform protective coating on the Li metal surface, whereas the impedance related to charge transfer across the interface begins to increase with further MLD cycles. In contrast, the bare Li cells begin to show a significant increase in overpotential by 50 cycles and begin short-circuiting after approximately 70 cycles.

The electrochemical performance of the Li@25ZrEG electrode was further probed at high current densities of 3 and 5 mA cm^{-2} (Figure 2 A,B). It can be seen that in the initial stages of cycling, the symmetrical cells with Li@25ZrEG show higher overpotential compared to those with bare Li. The larger overpotential likely arises from the charge transfer barrier at the interface between Li metal and the electrolyte. Nevertheless, it can be seen that although the overpotential is slightly higher, it has prolonged stability and lifetime. Furthermore, the Li@25ZrEG was pushed to a higher current density of 5 mA cm^{-2}. Similarly, the overpotential is higher for the coated Li metal in the initial stages but the prolonged cycling stability is far superior to the bare Li metal. The voltage profiles at the 10th, 50th and 100th cycles are displayed in Figure S4. The voltage profiles further indicate the stable plating/stripping behavior of Li@25ZrEG with minimal increase in overpotential. The peak overpotential of Li@25ZrEG can be seen to increase from ≈180 to ≈195 mV during the 10th to 100th cycle at 3 mA cm^{-2}, and a small decrease in overpotential is observed in the same region when cycled at 5 mA cm^{-2} after the initial stabilization cycles. In contrast, the bare Li cells undergo a much more rapid increase in overpotential compared to the protected Li, and the voltage profiles eventually become erratic due to dendritic Li formation. The gradual increase in overpotential during cycling may also indicate a tortuous pathway for Li ion diffusion caused by dead Li formation.[12] Moreover, the

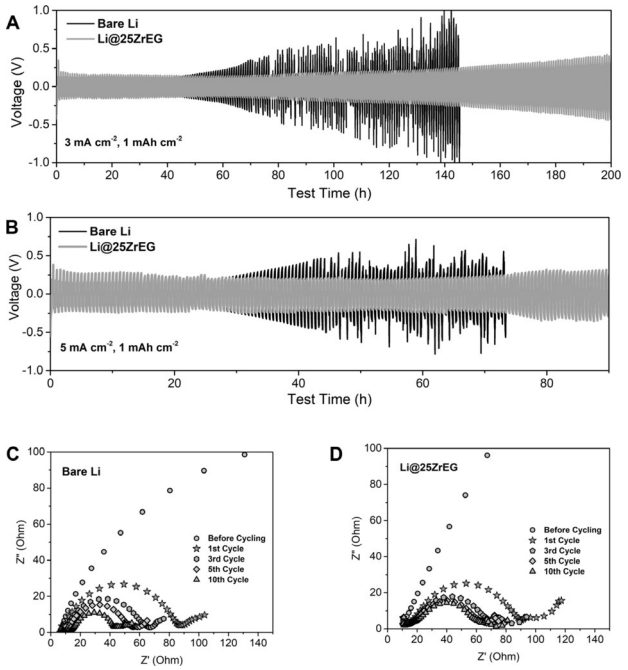

Figure 2. A) Li symmetrical cell cycling at a current density of 3 mA cm^{-2} and B) 5 mA cm^{-2}. C) EIS measurements of the bare Li symmetrical cell taken over the first 10 cycles and D) EIS measurements of the symmetrical cells with Li@25ZrEG taken over the first 10 cycles. All EIS measurements were conducted after cycling at a current density of 3 mA cm^{-2}.

ability of MLD zircone to operate at such high current densities is unmatched compared to other ALD/MLD-protected Li metal anodes including ZrO_2 and alucone (Figure S5).

The stabilizing effect of the zircone coating is further proven by in situ electrochemical impedance spectroscopy (Figure 2C,D). It can be seen that the overall impedance of the bare Li symmetrical cells cycled at 3 mA cm^{-2} continuously decrease from the 1st to 10th cycle without reaching a stabilized value. It is likely that the Li metal is unable to accommodate the strong Li^+ flux at such a high current density, which results in high surface area dendrite formation and a lower overall impedance. While lower impedances may be good for rate capability, it may also indicate significant side reactions with the electrolyte and surface instability, eventually leading to quicker cell failure. Alternatively, the cells assembled with Li@25ZrEG show a larger initial SEI resistance, which supports the larger overpotential observed in symmetrical cell cycling. However, it can be seen that the SEI and surface of the zircone-coated Li metal can be completely stabilized by the 3rd cycle, where little change in the overall impedance is observed in the following cycles. The results of the EIS measurements further support the ability of zircone to stabilize the Li metal surface at high current densities.

The surface morphology of the bare and protected Li metal anodes were further analyzed by scanning electron microscopy (SEM). It can be seen that the fabrication of Li@25ZrEG has little effect on the initial surface morphology of the Li surface compared to the pristine Li anode (Figure S6). However, after 30 cycles, the bare Li controls display significant dead Li formation on the surface with large cracks revealing a porous interior (Figure 3A,C). The non-uniform

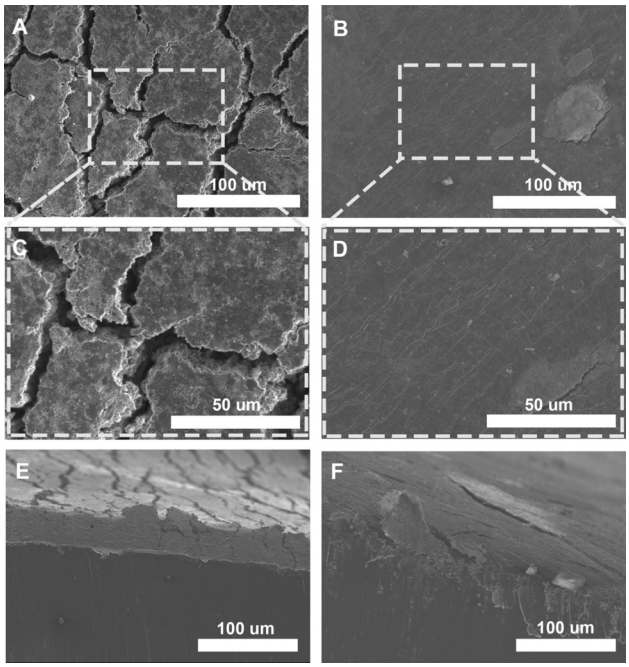

Figure 3. SEM images of bare Li and Li@25ZrEG electrodes after 30 cycles. A) Top view image of bare Li metal and C) magnified region. B) Top view image of Li@25ZrEG and D) magnified region. E) and F) cross-section SEM images of bare Li metal and Li@25ZrEG electrodes after 30 cycles, respectively.

Li ion flux to the surface of the unprotected Li may cause poor nucleation and inhomogeneous plating, leading to lower cycling efficiency and inactive Li deposits. Nevertheless, the zircone-protected Li metal shows a significant improvement in Li deposit uniformity and structural integrity (Figure 3B,D). Few cracks are observed in the Li@25ZrEG electrode and no dendrites are found, even at a high current density of 3 mA cm^{-2}. These results indicate that the zircone coating cannot only improve the mechanical integrity of the Li metal interface, but also increase Coulombic efficiency and enable uniform Li ion flux across the surface. Moreover, these results are further confirmed by the cross-sectional SEM images, where a significant dead Li layer ($\approx$40 um) is observed on the bare Li anode (Figure 3E) and only a thin passivating layer can be seen on the Li@25ZrEG electrode (Figure 3F).

Synchrotron-based in situ XAS is a powerful technique that utilizes a highly collimated X-ray beam to probe the density of unoccupied electronic states in atoms through excitation of core level electrons. While in-situ based XAS experiments for the study of battery materials and interfaces have become more popular in recent years,[13] the technique has yet to be applied for the study of the Li metal interface. The high flux and ability of synchrotron radiation to probe the local electronic structure of crystalline and amorphous

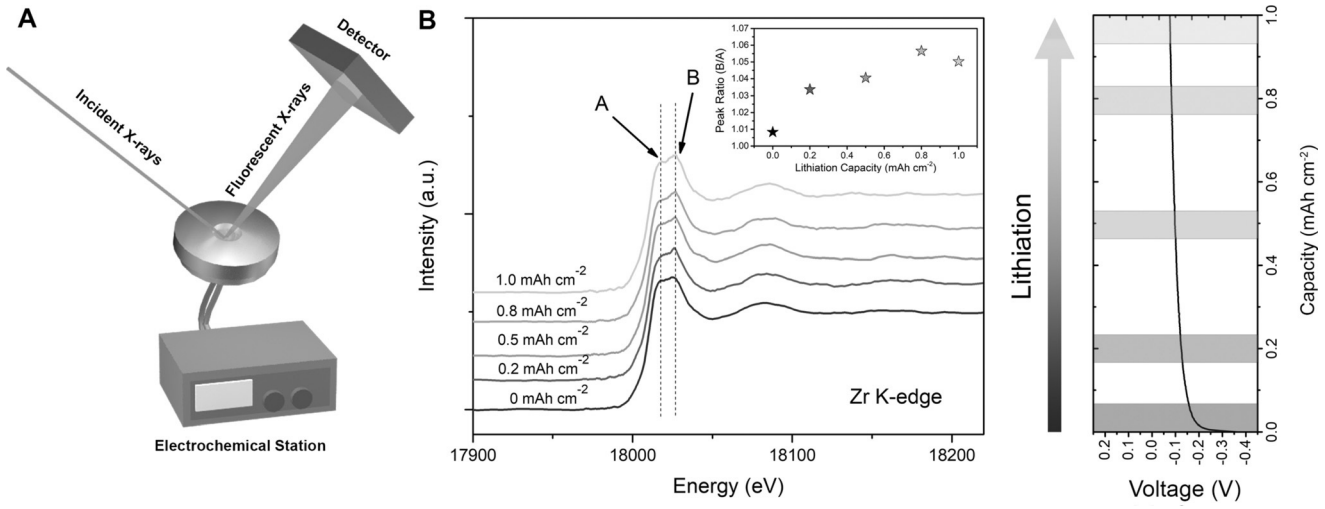

Figure 4. A) Image depicting the setup used to study the MLD zircone coating via in-situ XAS. B) In-situ Zr K-edge XANES during the first lithiation subcycle of the Li@25ZrEG electrode in a quasi symmetrical cell setup (Li@25ZrEG || Li). The inset image depicts the relative intensity ratio of peaks B/A. The voltage profile and corresponding points of measurement are displayed on the right.

materials at the atomic level makes it ideal for the analysis of interfacial coatings on Li metal. Here, we utilize in-situ XANES to study the Zr K-edge of MLD zircone on Li metal during the initial Li plating in a quasi-symmetric cell. A modified coin cell with a viewing port sealed by Kapton tape was utilized to enable X-rays to penetrate through the Li metal to the anode/electrolyte interface where the zircone film was present on one side of the quasi-symmetric cell (Figure 4 A). The initial state of the zircone coating on a Al_2O_3 wafer and Li metal can be seen in Figure S7 A. The coating on different substrates share similar features to various phases of crystalline ZrO_2, where the white line is split into two peaks and the ratio between them can be related to the coordination and bond length in the local Zr environment.[14]

However, it is evident that the electronic structure of the zircone is different depending on the substrate. On Al_2O_3, the Zr K-edge spectra displays a pre-edge feature starting at ≈17996 eV corresponding to a distortion of the local Zr structure which is related to the presence of non-centrosymmetric site symmetry. In contrast, the zircone coating on Li metal shows the absence of this pre-edge feature and the formation of a more prominent secondary white line peak (peak B) located at ≈18027 eV. It is likely that at some point after coating of the Li metal, the film becomes partially lithiated causing the observed change in the local electronic structure of Zr. Moreover, the average oxidation state of the Zr atoms on Li metal is found to be approximately 3.5^+, which may be a result of the partial electron withdrawing ability of the organic ligands and different molecular crosslinking structures between metal atoms (Figure S7 B). Further lithiation of the zircone coating on Li metal was observed in-situ during electrochemical cycling. Upon applying a constant current of 0.5 mA cm^{-2} and directing Li flux towards the coated Li anode, no significant change in the edge jump position can be observed, which suggests that the Zr center remains in an oxidized state and is not electrochemically reduced (Figure 4 B). However, the ratio between peaks A and B undergo subtle changes during the lithiation process. Shortly after the lithiation begins, the ratio of peaks B:A increase from ≈1.01 to 1.06. This change may be attributed to the distortion of the Zr local environment caused by Li transport through the film. The gradual nature of the change in the spectral features likely suggests that the film is initially subject to inhomogeneous chemical lithiation and the non-lithiated regions of the film become activated with continued Li plating. Moreover, it has been previously reported that the doublet white line feature observed in some Zr species becomes more pronounced with increasing Zr–O bond length, which could indicate uptake of Li in this instance.[15] This type of phenomenon can be supported by FEFF9 modelling of the lithiation of a similar Li_2ZrO_3 structure (Figure S8), in which Li insertion into the delithiated lattice causes a similar trend where the ratio of peaks B:A increase with further lithiation.

To demonstrate the effectiveness of MLD zircone for real applications, Li-O_2 full cells were assembled with Li@25ZrEG and a N-doped carbon nanotube/carbon paper composite cathode. Figure 5 A and 5 B present the full cell performances of Li-O_2 batteries with the protected and unprotected Li anodes, respectively. It quickly becomes evident that the batteries with Li@25ZrEG have significantly enhanced electrochemical stability and lifetime. Li-O_2 batteries suffer from dendritic Li formation, side-reactions with electrolyte, and oxygen species crossover which form high impedance Li_2O and LiOH layers on the surface of Li metal. Thus, it is expected that the zircone-coated Li can improve the stability and cycle life of Li-O_2 batteries based off previous air stability tests. The Li-O_2 system with a Li@25ZrEG anode shows outstanding stability for over 500 h with little change in voltage polarization (Figure 5 C,D). In contrast, the cell with bare Li is unstable and suffers from micro-short circuiting in less than 50 h. The high performance of the Li-O_2 batteries with zircone-protected Li metal can be supported by the

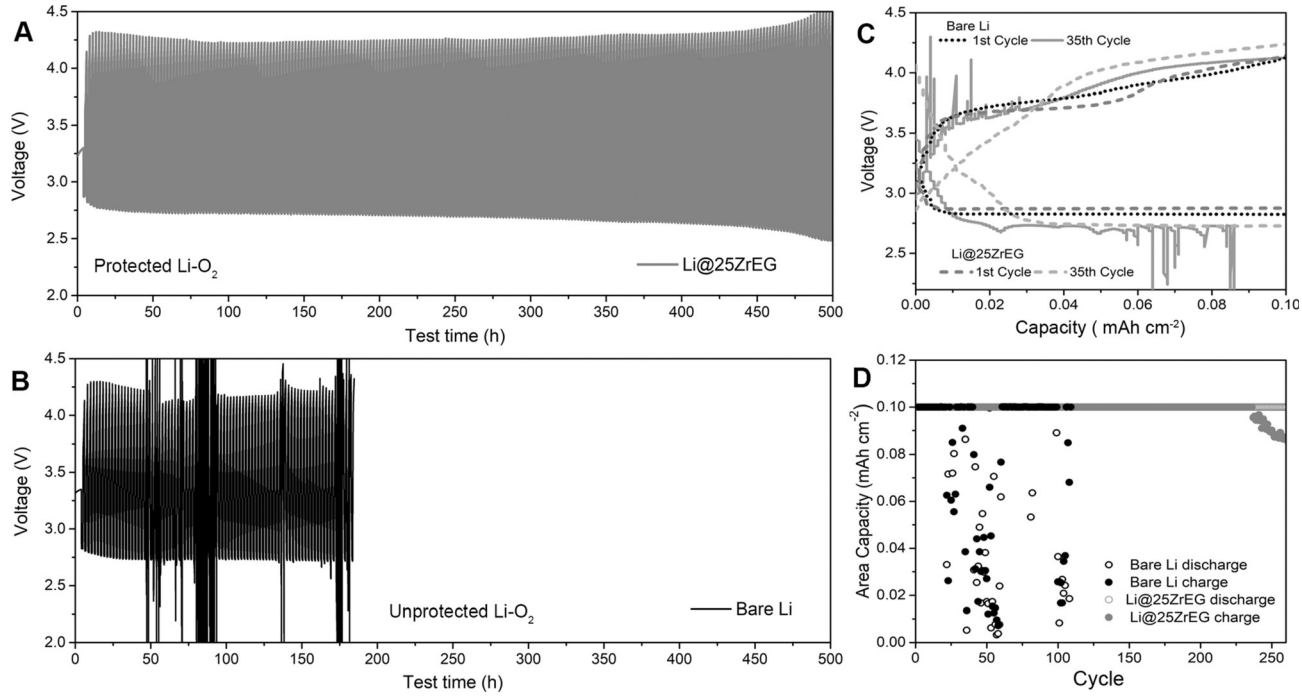

Figure 5. Electrochemical performance of Li-O_2 battery with a A) Li@25ZrEG anode and B) bare Li metal anode. C) Voltage profiles of Li-O_2 batteries with Li@Z5ZrEG and bare Li metal anodes at the 1st and 35th cycles. D) Charge/discharge capacity comparison of the protected/unprotected batteries during electrochemical cycling.

ability of the coating to improve the air stability of the anode, which is a necessity to achieve long-life metal air batteries.

In conclusion, Li metal treated with MLD zircone shows enhanced electrochemical stability and cycle life. The nanoscale coating not only shows significantly improved electrochemical performances over previous ALD/MLD coatings, but also acts as a physical/chemical barrier against O_2, making it suitable for Li-O_2 batteries. Moreover, in situ XAS was used for the first time to study an artificial SEI layer on Li metal, and the electrochemical stability and lithiation of MLD zircone was explored. These findings provide significant advancements in electrochemical performance, processability, and understanding of the effects of MLD coatings for high performance next-generation batteries.

Acknowledgements

This work was funded by the Natural Science and Engineering Research Council of Canada (NSERC), the Canada Research Chair Program (CRC), the Canada Foundation for Innovation (CFI), the University of Western Ontario (UWO), Ontario Research Fund (ORF) and General Motors R&D Center. Synchrotron characterization was performed at multiple facilities including the Canadian Light Source, which is supported by CFI, NSERC, CHIR, NRC, and the University of Saskatchewan. This research also used resources of the Advanced Photon Source, a U.S. Department of Energy (DOE) Office of Science User Facility operated for the DOE Office of Science by Argonne National Laboratory under Contract No. DE-AC02-06CH11357. We would also like to acknowledge the help of beamline staff at beamline 44A of the Taiwan Photon Source (TPS).

Conflict of interest

The authors declare no conflict of interest.

Keywords: artificial SEI · electrochemistry · energy storage · Li metal anode · molecular layer deposition

How to cite: *Angew. Chem. Int. Ed.* **2019**, *58*, 15797–15802
Angew. Chem. **2019**, *131*, 15944–15949

[1] a) Z. Liu, Y. Qi, Y. X. Lin, L. Chen, P. Lu, L. Q. Chen, *J. Electrochem. Soc.* **2016**, *163*, A592–A598; b) D. Lu, Y. Shao, T. Lozano, W. D. Bennett, G. L. Graff, B. Polzin, J. Zhang, M. H. Engelhard, N. T. Saenz, W. A. Henderson, P. Bhattacharya, J. Liu, J. Xiao, *Adv. Energy Mater.* **2015**, *5*, 1400993.

[2] a) S. Li, M. Jiang, Y. Xie, H. Xu, J. Jia, J. Li, *Adv. Mater.* **2018**, *30*, 1706375; b) Z. Liang, D. Lin, J. Zhao, Z. Lu, Y. Liu, C. Liu, Y. Lu, H. Wang, K. Yan, X. Tao, Y. Cui, *Proc. Natl. Acad. Sci. USA* **2016**, *113*, 2862–2867.

[3] a) P. Bai, J. Li, F. R. Brushett, M. Z. Bazant, *Energy Environ. Sci.* **2016**, *9*, 3221–3229; b) D. Lin, Y. Liu, Y. Cui, *Nat. Nanotechnol.* **2017**, *12*, 194–206.

[4] a) K. R. Adair, M. Iqbal, C. Wang, Y. Zhao, M. N. Banis, R. Li, L. Zhang, R. Yang, S. Lu, X. Sun, *Nano Energy* **2018**, *54*, 375–382; b) C. P. Yang, Y. X. Yin, S. F. Zhang, N. W. Li, Y. G. Guo, *Nat. Commun.* **2015**, *6*, 8058; c) J. Xie, J. Wang, H. R. Lee, Y. Cui, *Sci. Adv.* **2018**, eaat5168.

[5] a) X.-Q. Zhang, X.-B. Cheng, X. Chen, C. Yan, Q. Zhang, *Adv. Funct. Mater.* **2017**, *27*, 1605989; b) F. Ding, W. Xu, G. L. Graff, J.

Zhang, M. L. Sushko, X. Chen, Y. Shao, M. H. Engelhard, Z. Nie, J. Xiao, X. Liu, P. V. Sushko, J. Liu, J. G. Zhang, *J. Am. Chem. Soc.* **2013**, *135*, 4450 – 4456.
[6] a) J. Lopez, A. Pei, J. Y. Oh, G. N. Wang, Y. Cui, Z. Bao, *J. Am. Chem. Soc.* **2018**, *140*, 11735 – 11744; b) X. Liang, Q. Pang, I. R. Kochetkov, M. S. Sempere, H. Huang, X. Sun, L. F. Nazar, *Nat. Energy* **2017**, *2*, 17119.
[7] a) Y. Sun, Y. Zhao, J. Wang, J. Liang, C. Wang, Q. Sun, X. Lin, K. R. Adair, J. Luo, D. Wang, R. Li, M. Cai, T. K. Sham, X. Sun, *Adv. Mater.* **2019**, *31*, 1806541; b) Y. Zhao, L. V. Goncharova, Q. Sun, X. Li, A. Lushington, B. Wang, R. Li, F. Dai, M. Cai, X. Sun, *Small Methods* **2018**, *2*, 1700417; c) E. Kazyak, K. N. Wood, N. P. Dasgupta, *Chem. Mater.* **2015**, *27*, 6457 – 6462; d) P. K. Alaboina, S. Rodrigues, M. Rottmayer, S.-J. Cho, *ACS Appl. Mater. Interfaces* **2018**, *10*, 32801 – 32808.
[8] B. H. Lee, V. R. Anderson, S. M. George, *Chem. Vap. Deposition* **2013**, *19*, 204 – 212.
[9] S. M. George, B. H. Lee, B. Yoon, A. I. Abdulagatov, R. A. Hall, *J. Nanosci. Nanotechnol.* **2011**, *11*, 7948 – 7955.
[10] X. Shen, Y. Li, T. Qian, J. Liu, J. Zhou, C. Yan, J. B. Goodenough, *Nat. Commun.* **2019**, *10*, 900.
[11] D. W. Choi, M. Yoo, H. M. Lee, J. Park, H. Y. Kim, J. S. Park, *ACS Appl. Mater. Interfaces* **2016**, *8*, 12263 – 12271.
[12] K.-H. Chen, K. N. Wood, E. Kazyak, W. S. LePage, A. L. Davis, A. J. Sanchez, N. P. Dasgupta, *J. Mater. Chem. A* **2017**, *5*, 11671 – 11681.
[13] J. Lu, T. Wu, K. Amine, *Nat. Energy* **2017**, *2*, 17011.
[14] P. Ghosh, K. P. Priolkar, A. Patra, *J. Phys. Chem. C* **2007**, *111*, 571 – 578.
[15] R. B. Greegor, K. Y. Blohowiak, J. H. Osborne, K. A. Krienke, J. T. Cherian, F. W. Lytle, *J. Sol-Gel Sci. Technol.* **2001**, *20*, 35 – 50.

Manuscript received: June 21, 2019
Revised manuscript received: August 6, 2019
Accepted manuscript online: August 10, 2019
Version of record online: September 13, 2019

